

## **Supporting Information**

### **Unusual Enhancement in the Electroreduction of Oxygen by NiCoPt by Surface Tunability through Potential Cycling**

Moorthi Lokanathan,<sup>ab</sup> Indrajit M. Patil,<sup>ac</sup> Alhasan Kabiru Usman,<sup>c</sup> Anita Swami,<sup>c</sup> Pravin Walke,<sup>d</sup> M. Navaneethan<sup>e</sup> and Bhalchandra Kakade<sup>ac\*</sup>

SRM Research Institute,<sup>a</sup> SRM University, Kattankulathur - 603 203, Chennai (India)

Department of Physics and Nanotechnology,<sup>b</sup> SRM University, Kattankulathur - 603 203, Chennai (India)

Department of Chemistry,<sup>c</sup> SRM University, Kattankulathur - 603 203, Chennai (India)

National Centre for Nanosciences and Nanotechnology,<sup>d</sup> University of Mumbai, Mumbai - 400098 (India)

Research Institute of Electronics,<sup>e</sup> Shizuoka University, 3-5-1 Johoku, Naka-Ku, Hamamatsu, Shizuoka 432-8011, Japan.

Fax: (+91) 44-2745 6702; Tel: (+91) 44-2741 7920.

\*Corresponding author E-mail: [bhalchandrakakade.a@res.srmuniv.ac.in](mailto:bhalchandrakakade.a@res.srmuniv.ac.in)

**Table S1.** The activity comparison of various NCP catalysts

Catalyst	ECSA ( $\text{m}^2/\text{g}_{\text{Pt}}$ )	$I_{\text{m}} (\text{mA}/\text{mg}_{\text{Pt}})$	$I_{\text{s}} (\text{mA}/\text{cm}^2_{\text{Pt}})$
NCP6/C	26.48	141.46	534.07
NCP8/C	13.169	96.24	729.97
<b>NCP10/C</b>	<b>68.18</b>	<b>505.24</b>	<b>741.31</b>
NCP16/C	21.7	271.36	651.709

**Table S2.** Comparison of electrochemical activity of Pt-based ternary alloy catalysts

S. No.	Catalyst	ECSA ( $\text{m}^2/\text{g}_{\text{Pt}}$ )		MA (A/ $\text{mg}_{\text{Pt}}$ )		Normalized MA loss or gain @ 0.9 V (%) /cycles (1k=1000)			Ref.
		Before stability	After stability	Before stability	After stability	Loss (%)	Gain (%)	Cycles (k)	
1	Pt65Ir11Co24/C – 400 °C	70	25	0.41	0.06	85		20k	1
2	Pt-Rh-Ni/C	N/A	N/A	0.82	1.14		39	4k	2
3	Pt-Rh-Ni/C	N/A	N/A	0.82	0.72	12.2		8k	2
4	Pt-Rh-Ni/C	N/A	N/A	0.82	0.32	61		30k	2
5	Pt3Ni-Fe/C (13 nm)	28.9	27.46	0.37	N/A	25		16k	3
6	Mo-Pt3Ni/C	67.7	N/A	6.98	6.6	5.5		8k	4
7	Pt2CuNi/C	35.3	36.85	2.35	1.91	18.7		4k	5
8	Pt2CuNi/C	35.3	N/A	2.35	1.60	31.9		10k	5
9	PtCu3Co	112	N/A	0.37	N/A	N/A	N/A	N/A	6
10	PtCuCo3	111	N/A	0.49	N/A	N/A	N/A	N/A	6
11	Pt30Ni51Co19 – 1 step	8.6	N/A	N/A	N/A	47		4k	7
12	Pt48Ni27Co25 – 2 step	3	N/A	N/A	N/A	51		4k	7
13	Pt36Ni15Co49/C – 400 °C	56.6	N/A	0.56	0.11	80.4		10k	8
14	Pt36Ni15Co49/C – 700 °C	48.0	N/A	0.73	0.15	79.5		10k	8
15	Pt36Ni15Co49/C – 926 °C	47.7	N/A	0.88	0.21	76.1		10k	8
16	Ni@Au@PtNi/C	51	50	0.38	0.35	<10		10k	9
17	PtCoMn	N/A	N/A	2.1	1.0	52.4		1.08k	10
18	PtCoMn	N/A	N/A	N/A	0.2.16	71.4		2.16k	10
19	Pt2FeCo/C – L10	2.6	3.2	0.51	0.4	21.6		2.16k	11

20	Pt6FeCo/C –L12	3.45	2	0.27	0.17	37.0		5k	11
21	Pt2FeCo/C – 800 °C	60	52	0.505	0.38	24.8		5k	12
22	Pt2FeCo/C	4.51	3.87	0.0665	0.0286	57		5k	13
23	Pt2FeNi/C	4.25	5.12	0.0684	0.0286	58.2		2k	13
24	Pt2CoNi/C	3.97	3.10	0.0634	0.0298	53		2k	13
25	PtNiFe nanocubes	70.4	N/A	0.00534	0.00498	6.7		1k	14
26	PtNiFe octrahedran	73.3	N/A	0.0042	N/A	N/A		N/A	14
27	PtNiFe polyhedran	68.5	N/A	0.00467	N/A	N/A		N/A	14
28	PtNiFe nanowire	69.3	N/A	0.00399	N/A	N/A		N/A	14
29	Pt-Ni-Ir/C	49.45	44.51	0.511	0.337	34		10k	15
30	Fct-PtFeCu	43	36	0.5	0.38	24		10k	16
31	Fct-PtFeCo	52	37	0.48	0.32	33.3		10k	16
<b>30</b>	<b>PtNiCo/C</b>	<b>68.1</b>	<b>54.7</b>	<b>0.5052</b>	<b>0.5811</b>		<b>15</b>	<b>10k</b>	<b>This work</b>
<b>31</b>	<b>PtNiCo/C</b>	<b>68.1</b>	<b>52.3</b>	<b>0.505</b>	<b>0.6557</b>		<b>29.8</b>	<b>20k</b>	<b>This work</b>
<b>32</b>	<b>PtNiCo/C</b>	<b>68.1</b>	<b>51.5</b>	<b>0.505</b>	<b>0.6957</b>		<b>37.7</b>	<b>30k</b>	<b>This work</b>

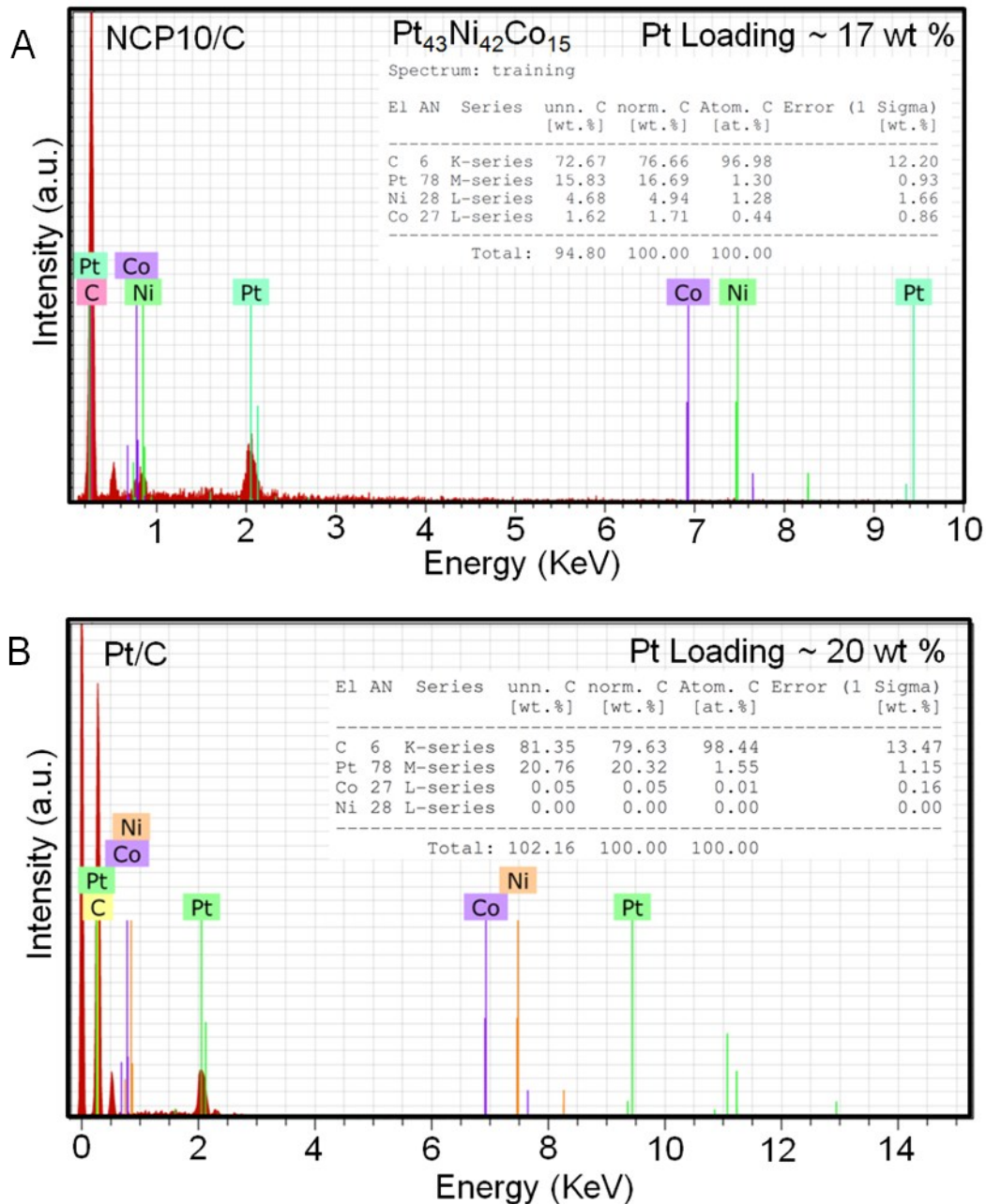


**Figure S1.** EDX patterns of (A) The NCP10/C catalyst and (B) commercial Pt/C.

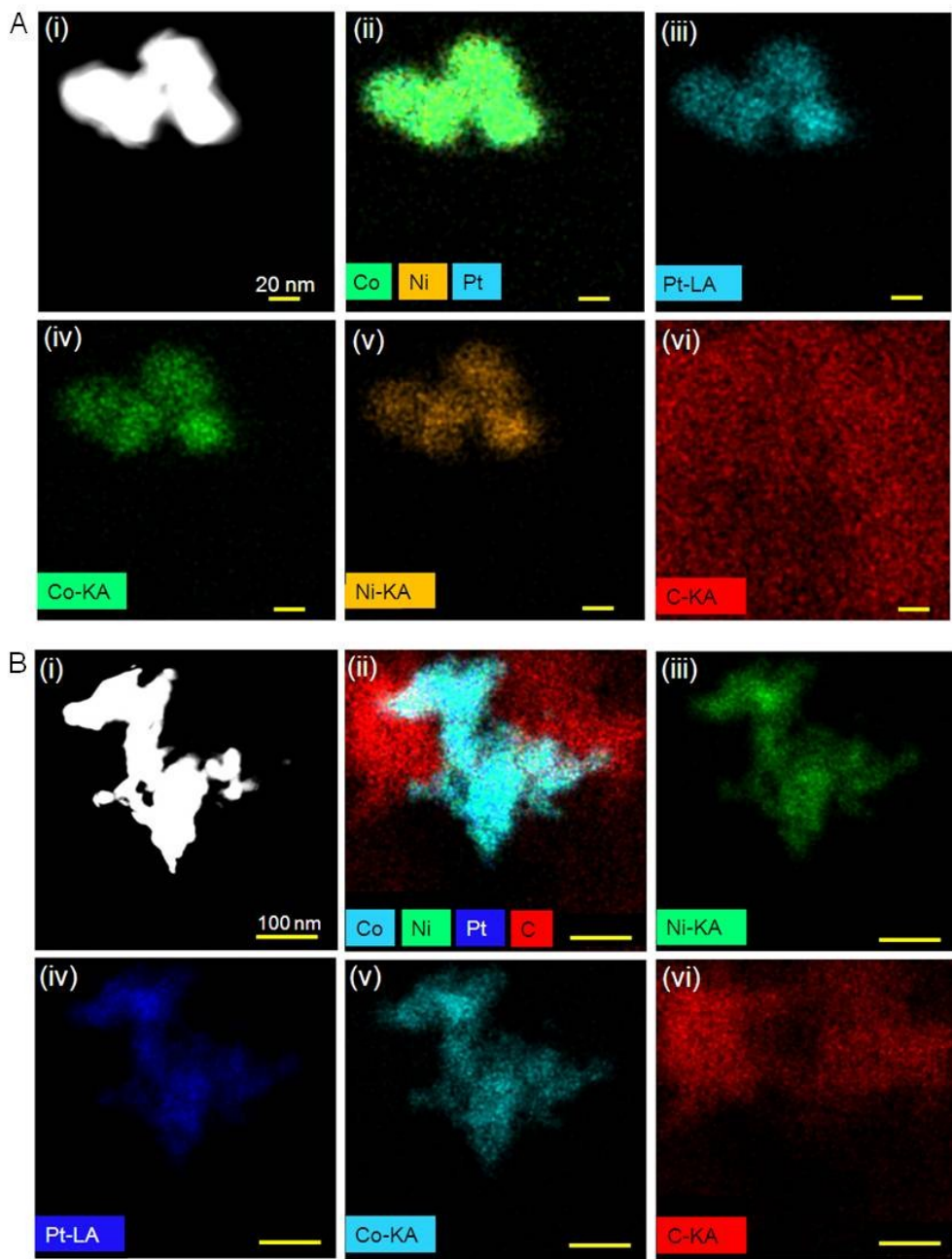


**Figure S2.** A (i) HAADF-STEM image of a NCP10/C before stability test. (ii-vi) EDS elemental mapping distributions for (ii) Co, Ni and Pt;(iii) Pt;(iv) Co; (v) Ni and (vi) C. B (i) HAADF-STEM image of a NCP10/C after stability test. (ii-vi) EDS elemental mapping distributions for (ii) Co, Ni, Pt and C;(iii) Ni;(iv) Pt;(v) Co and (vi) C.

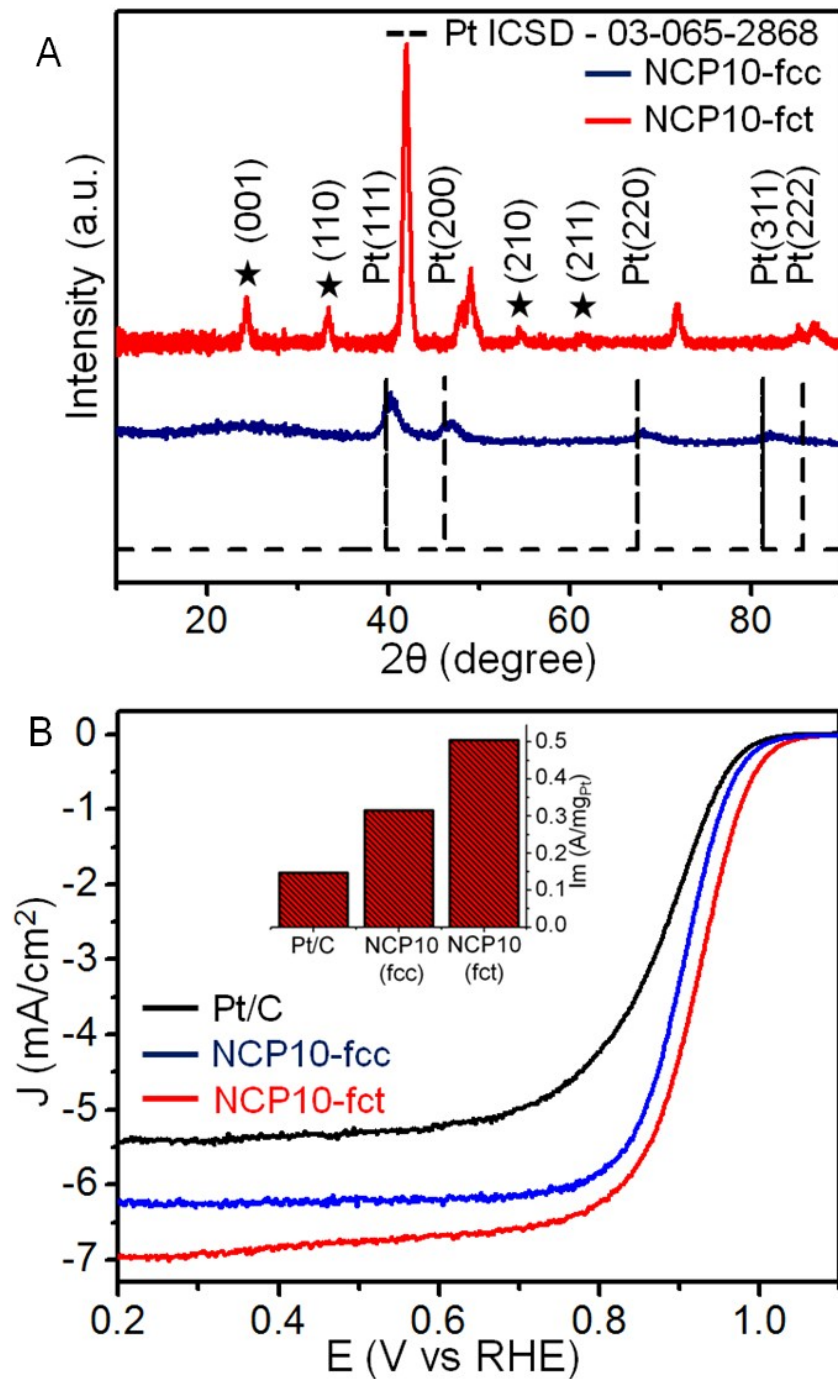


**Figure S3.** (A) Comparative XRD pattern of fcc and fct structure of NCP10/C catalyst with Pt ICSD-03-065-2868. (B) Linear sweep voltammograms of NCP10(fcc), NCP10(fct) and Commercial Pt/C catalyst, recorded in the presence of O<sub>2</sub>-saturated 0.1 M HClO<sub>4</sub> at 25°C at a sweep rate of 10 mVs<sup>-1</sup> and rotation rate of 1600 rpm and inset shows the their comparative mass activity (Im).

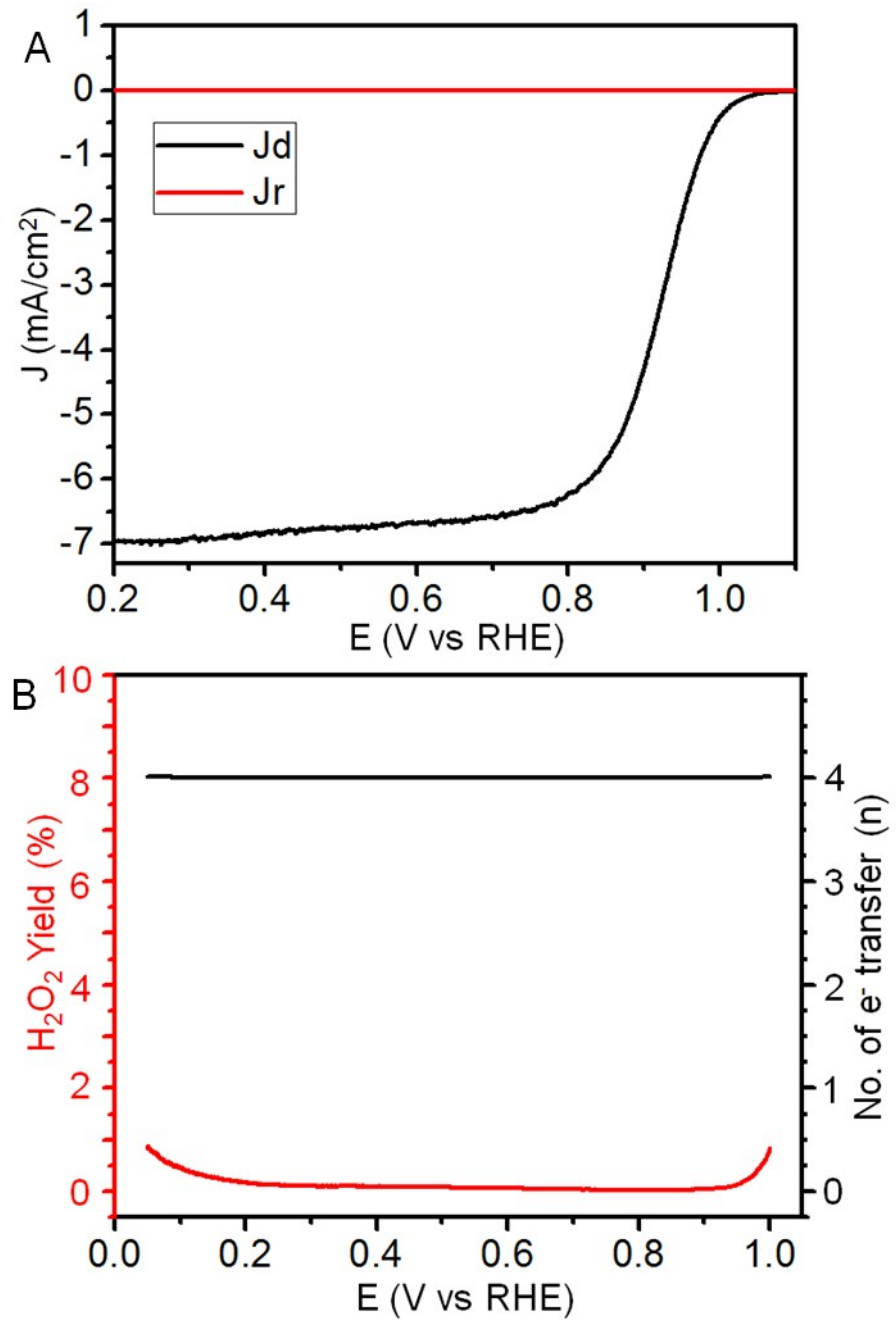


**Figure S4.** (A) Rotating ring-disk electrode (RRDE) voltammograms of NCP10/C catalyst. The disk electrode was scanned at a rate of  $10 \text{ mV s}^{-1}$  with  $1600 \text{ rpm}$  and the ring potential was kept constant at  $1.3 \text{ V}$  vs. RHE. (B)  $\text{H}_2\text{O}_2$  percentage yield and no. of electron transfer during the reaction.

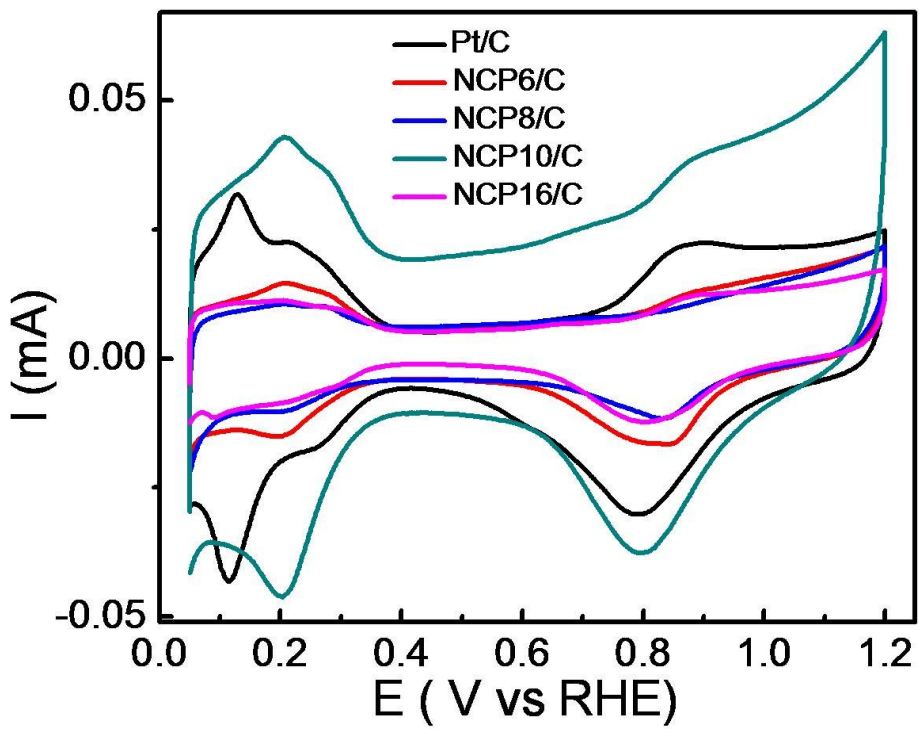


**Figure S5.** The Cyclic voltammograms comparison of NCP6/C, NCP8/C, NCP10/C, NCP16/C electrocatalyst with Commercial Pt/C catalyst, recorded in the presence of  $N_2$ -saturated 0.1 M  $HClO_4$  at a sweep rate of  $20\text{ mVs}^{-1}$ .

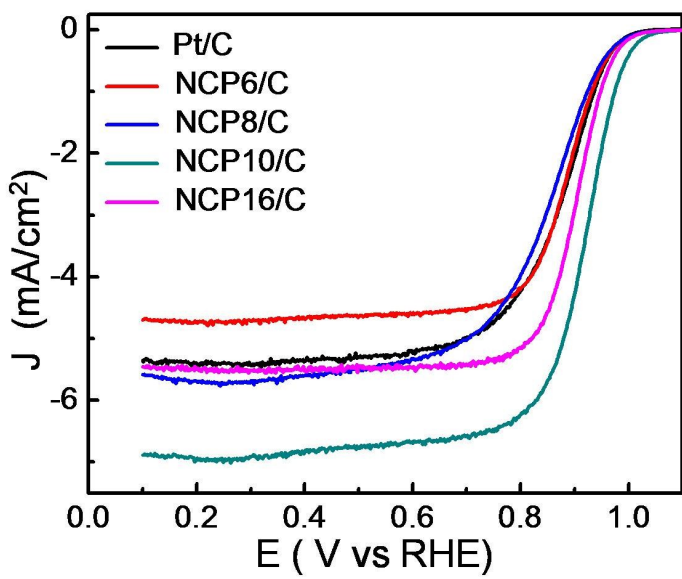


**Figure S6.** Linear sweep voltammograms of NCP6/C, NCP8/C, NCP10/C, NCP16/C and Commercial Pt/C catalyst, recorded in the presence of O<sub>2</sub>-saturated 0.1 M HClO<sub>4</sub> at 25°C at a sweep rate of 10 mVs<sup>-1</sup> and rotation rate of 1600 rpm

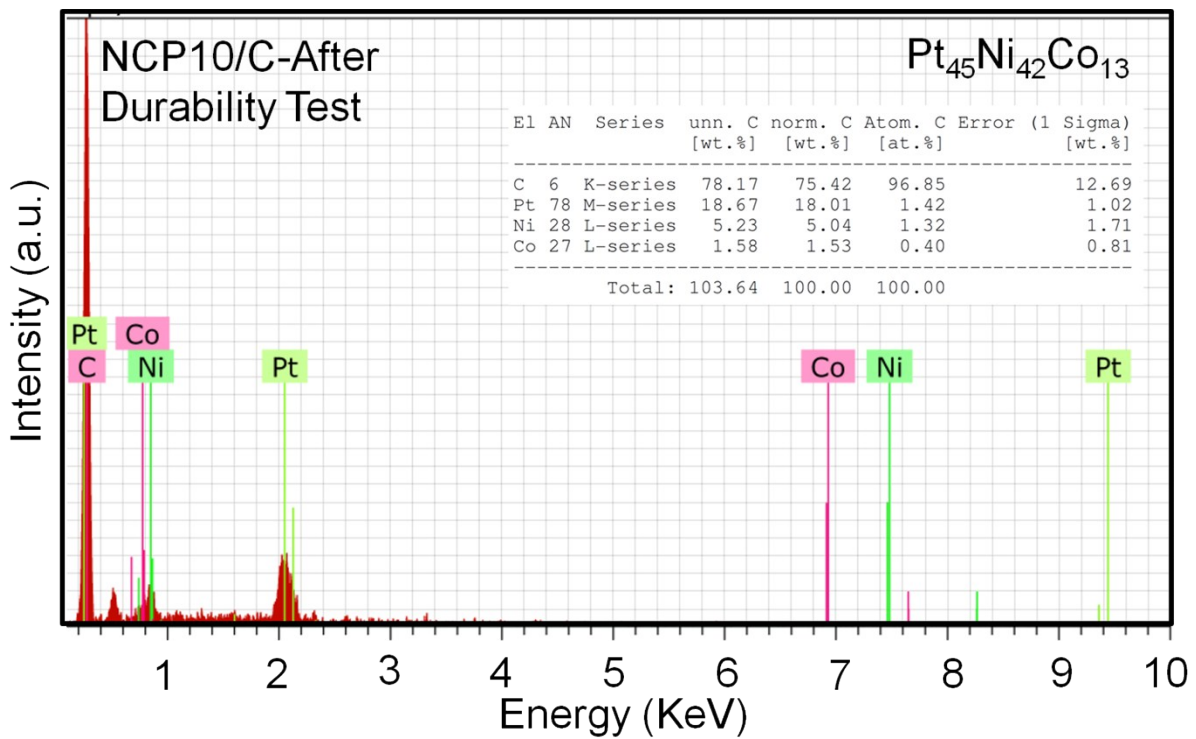


**Figure S7.** EDX patterns of the NCP10/C catalyst after 30 k durability cycles.

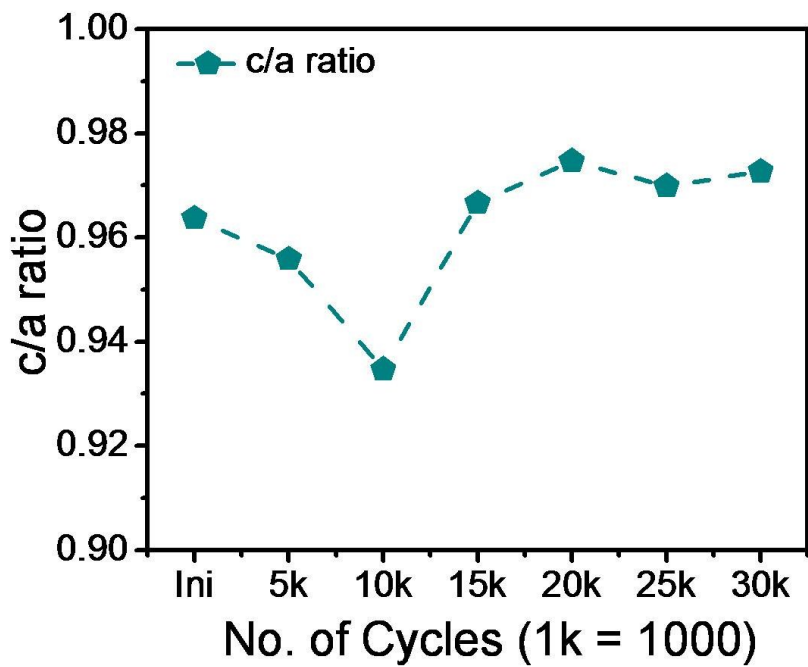


**Figure S8.** The c/a ratio of the NCP10/C catalyst calculated from the XRD pattern after different stability cycles.

## REFERENCES:

1. R. Loukrakpam, B. N. Wanjala, J. Yin, B. Fang, J. Luo, M. Shao, L. Protsailo, T. Kawamura, Y. Chen and V. Petkov, *ACS Catalysis*, 2011, **1**, 562-572.
2. V. Beermann, M. Gocyla, E. Willinger, S. Rudi, M. Heggen, R. E. Dunin-Borkowski, M.-G. Willinger and P. Strasser, *Nano letters*, 2016, **16**, 1719-1725.
3. Y. Li, F. Quan, L. Chen, W. Zhang, H. Yu and C. Chen, *RSC Advances*, 2014, **4**, 1895-1899.
4. X. Huang, Z. Zhao, L. Cao, Y. Chen, E. Zhu, Z. Lin, M. Li, A. Yan, A. Zettl and Y. M. Wang, *Science*, 2015, **348**, 1230-1234.
5. C. Zhang, W. Sandorf and Z. Peng, *ACS Catalysis*, 2015, **5**, 2296-2300.
6. R. Srivastava, P. Mani, N. Hahn and P. Strasser, *Angewandte Chemie International Edition*, 2007, **46**, 8988-8991.
7. R. M. Arán-Ais, F. Dionigi, T. Merzdorf, M. Gocyla, M. Heggen, R. E. Dunin-Borkowski, M. Gliech, J. Solla-Gullón, E. Herrero and J. M. Feliu, *Nano letters*, 2015, **15**, 7473-7480.
8. B. N. Wanjala, R. Loukrakpam, J. Luo, P. N. Njoki, D. Mott, C.-J. Zhong, M. Shao, L. Protsailo and T. Kawamura, *The Journal of Physical Chemistry C*, 2010, **114**, 17580-17590.
9. Y. Kang, J. Snyder, M. Chi, D. Li, K. L. More, N. M. Markovic and V. R. Stamenkovic, *Nano letters*, 2014, **14**, 6361-6367.
10. M. Ishida and K. Matsutani, *ECS Transactions*, 2014, **64**, 107-112.
11. T. Tamaki, A. Minagawa, B. Arumugam, B. A. Kakade and T. Yamaguchi, *Journal of Power Sources*, 2014, **271**, 346-353.
12. B. Arumugam, B. A. Kakade, T. Tamaki, M. Arao, H. Imai and T. Yamaguchi, *RSC Advances*, 2014, **4**, 27510-27517.
13. M. T. Nguyen, R. H. Wakabayashi, M. Yang, H. D. Abruña and F. J. DiSalvo, *Journal of Power Sources*, 2015, **280**, 459-466.
14. S.-W. Chou, J.-J. Shyue, C.-H. Chien, C.-C. Chen, Y.-Y. Chen and P.-T. Chou, *Chemistry of Materials*, 2012, **24**, 2527-2533.

15. T. Yang, G. Cao, Q. Huang, Y. Ma, S. Wan, H. Zhao, N. Li, F. Yin, X. Sun and D. Zhang, *Journal of Power Sources*, 2015, **291**, 201-208.
16. B. Arumugam, T. Tamaki and T. Yamaguchi, *ACS applied materials & interfaces*, 2015, **7**, 16311-16321.